A General Segmentation Scheme for Contouring Kidney Region in Ultrasound Kidney Images using Improved Higher Order Spline Interpolation

K. Bommanna Raja, M.Madheswaran, K.Thyagarajah

Abstract—A higher order spline interpolated contour obtained with up-sampling of homogenously distributed coordinates for segmentation of kidney region in different classes of ultrasound kidney images has been developed and presented in this paper. The performance of the proposed method is measured and compared with modified snake model contour, Markov random field contour and expert outlined contour. The validation of the method is made in correspondence with expert outlined contour using maximum co-ordinate distance, Hausdorff distance and mean radial distance metrics. The results obtained reveal that proposed scheme provides optimum contour that agrees well with expert outlined contour. Moreover this technique helps to preserve the pixels-of-interest which in specific defines the functional characteristic of kidney. This explores various possibilities in implementing computer-aided diagnosis system exclusively for US kidney images.

Keywords—Ultrasound Kidney Image – Kidney Segmentation – Active Contour – Markov Random Field – Higher Order Spline Interpolation

I. INTRODUCTION

ULTRASONIC imaging gained widespread acceptance to visualize the organs of human abdominal cavity [1-5,7-13,24] in the recent years. Remarkable growth in such imaging technique and the use of computers to process the image data, results in an explosion in the number and importance of ultrasound (US) images stored in the most of the hospitals. In general diagnostic studies of US images are subjective and the resultant performance suffers from intra- and inter-observer variability. Unlike all imaging modalities,

K.Bommanna Raja is presently with the Centre of Research and Development, Department of Electronics and Communication Engineering, PSNA College of Engineering and Technology, Dindigul – 624 622, TamilNadu, INDIA, phone: +91-451-2554032, fax: +91-451-2554249, e-mail: bommanna_raja @psnacet.org.

M.Madheswaran is currently with the Centre for Advanced Research, Department of Electronics and Communication Engineering, Muthyammal Engineering College, Rasipuram – 637 408, TamilNadu, INDIA, phone: +91-4287-226837, fax: +91-4287-226537, e-mail: madhi_eswaran@yahoo.co.in

K.Thyagarajah is with the Centre of Research and Development, Department of Electronics and Communication Engineering, PSNA College of Engineering and Technology, Dindigul – 624 622, TamilNadu, INDIA, phone: +91-451-2554262, fax: +91-451-2554249, e-mail: contact @psnacet.org.

US imaging is subject to a number of artifacts that degrade image quality and compromise diagnostic confidence [3]. The major performance limiting factor in visual perception of US imaging is a multiplicative noise called speckle that makes the signal or lesion difficult to detect [4,5]. Also other factors that compounds are viewing distance, display size, resolution, brightness, contrast, sharpness, colorfulness and naturalness [6]. These constraints limit the possibility of segmentation of kidney region and the extraction of kidney features that helps to evaluate the functional characteristic objectively.

Many research papers on segmentation of kidney region in US images have been published using various methodologies in the recent past. Bakker *et. al.*[7] determined the in-vitro kidney volume using an ellipsoidal method in which manual adjustment of an ellipse template was made over the pre-assumed external boundary of the kidney to estimate the volume. Semi-automatic segmentation method was also reported by Matre *et. al.*[8] for in-vitro kidney. In these methods the contour estimation was made for in-vitro kidney, but in real clinical situation the kidney is in-vivo. Classical segmentation methods are fast and useful only for simple and controlled situation [9]. As US kidney images are noisy and have poor signal-to-noise ratio, robust method that makes use of *a-priori* information to compensate for such difficulty may be used as an alternative. Jun xie *et.al.* [10] developed a semi-automatic segmentation frame work using both texture and shape priors for kidney contour estimation from noisy US image. A novel approach for contour detection of human kidneys from US images was also proposed by Marcos Martin-Fernendz *et.al.* [11]. But these semi-automatic schemes require either a *prior* knowledge of image in terms of shape and features, which is used to form a smooth contour or need a predefined template for unsupervised deformation. Abouzar Eslami *et.al.* [12,13] concerned in particular a cystic kidney and developed an automatic approach for renal cyst segmentation from US images. This method is faster and also non-iterative with better accuracy.

The semi-automatic or automatic segmentation procedures suggested so far deals with contouring the kidney region by extracting localized features that reflect the region property. Though the performance of the methods in contouring the kidney region is well appreciated, they fail to formulate a generalized scheme by considering various kidney categories.

World Academy of Science, Engineering and Technology
International Journal of Electronics and Communication Engineering
Vol:2, No:1, 2008

Unless a common method for contour estimation irrespective of kidney category exits, the implementation of a computer-aided diagnosis (CAD) system may not be possible. Mostly the normal kidney images have been considered except [12,13] where the cystic kidneys have been taken for implementation. Due to the presence of speckle noise and other constraints establishing the general segmentation scheme for different classes of kidney is difficult and so far not been reported.

In this paper, a reliable semi-automatic segmentation scheme using a higher order spline interpolated contour obtained with up-sampling of homogenously distributed coordinates has been proposed. Uniqueness of this method lies in achieving the contour for different highly reported kidney classes namely normal (NR), medical renal diseases (MRD) and cortical cyst (CC).

II. METHODS

A. Image data acquisition

The images used for the analysis are acquired from two types of scanning systems namely, ATL HDI 5000 curvilinear probe with transducer frequency range of 3 – 6 MHz and Wipro GE LOGIC 400 curvilinear probe with transducer frequency range of 3 – 5 MHz. As the sonographic evaluation is made based on the distribution of echogenity that reflects tissue characteristics, for better echo visualization the longitudinal cross section of kidney is taken to include renal sinus, medulla and cortex regions as suggested by the experts. This also ensures better visual interpretation of the normal and diseased kidney. The transducer frequency is fixed at 4 MHz. In total, 150 images with 50 images in each category are obtained from male and female subjects of age 46 (±12), 50 (±18) and 54 (±13) years. The images of both right and left kidneys are considered for the analysis. The kidney diseases are usually categorized as hereditary, congenital or acquired. The most common hereditary disorder is cystic diseases which includes simple renal cyst and complex renal cyst or poly cyst. The kidneys affected with these diseases are considered under CC category. The sonographic features of renal cyst include a well defined mass lesion, smooth wall and circular hypo echoic mass with good through transmission. Any congenital or acquired kidney diseases typically cause renal infection and/or destruction of kidney tissues that may lead to end stage chronic renal failure are considered under MRD category. Due to tissue destruction, anatomical separation between renal sinus, medulla and cortex becomes difficult. The sonographic evaluation shows hyper echoic kidney region with increased cortical echogenity and differentiation between cortex and collecting system is poor. The sample US kidney images of NR, MRD and CC are shown in the Fig 1. It can be seen that ultrasound shows appreciable renal border in all three cases, but internally due to pathology involved the echogenity varies in diseased kidneys (MRD and CC) when compare to NR.

B. Segmentation of kidney region

In this section the different segmentation methods used for contouring the kidney region is discussed in detail. Any segmentation scheme should not only contour the kidney region but must involve less complexity in achieving it. Also the scheme must concern with minimal expert intervention and be reliable for segmentation of different categories of kidney. In the present study four types of segmentation schemes are used for contouring namely expert outlined contour (EOC), modified snake model contour (MSMC), Markov random field contour (MRFC) and proposed higher order spline interpolated contour obtained with up-sampling of homogenously distributed coordinates (*i*-HSIC). Based on the performance analysis it will be shown that proposed method agrees well with the EOC and may be used for different kidney categories. The entire implementation is made by using MATLAB 6.1 software.

Fig. 1 a. Normal image of male with age 38 years, b. Medical renal diseases image of male with age 45 years and c. Cortical polycystic disease image of female with age 51 years.

World Academy of Science, Engineering and Technology
International Journal of Electronics and Communication Engineering
Vol:2, No:1, 2008

The EOC is obtained for each image by allowing the experts to draw the manual outline through visual inspection over the identified boundary by moving the cursor using mouse. For an image six experts are requested to form an outline individually to account the inter-expert variability. As the segmentation schemes reported for contouring the kidney region in literatures not concern about the different kidney categories, a common gold-standard contour or method is not available. Hence the average of the multiple experts' outline is derived by using the averaging procedure suggested by Vikram Chalana and Yongmin Kim [14]. The resultant outline is termed as EOC and may be used as a gold-standard for comparative study of contours formed by MSMC, MRFC and *i*-HSIC. The second segmentation scheme is an enhanced form of classical active contour approach in particular, *snake model* proposed by Kass *et.al.* [15]. The modification of snake model contour has been made as suggested by Cohen [16]. The contour achieved with this scheme is named as MSMC. Here the initial ellipse is drawn manually either inside or outside the kidney region. This will act as a seed contour that will deflate for negative deformation function and inflate for positive deformation function according to the deflation or inflation force controlled by the image gradient. As the positive deformation function that inflates is more appropriate for the US kidney images [11], the same has been used for the present study. The MRFC is obtained by formulating the problem in Bayesian probabilistic frame work and make use of Markov random fields (MRFs) [11,17]. Here, the deformation of predefined template has been incorporated using MRFs to get optimum kidney contour. The template is manually adjusted to approximately match the kidney boundary and then smoothly deformed using the model. This deformation procedure is fully unsupervised. The prior distributions will model the knowledge about the contours and data-driven likelihood terms will describe the image statistics related to the contour in search. The maximum *a posteriori* (MAP) estimation under MRFs model gives rise to the optimum contour. As mentioned, this model requires a template from which deformation starts taking place. Formulation of template is very simple, on the selected image the center point is clicked-in with the mouse. Then a built-in routine form a projection of straight lines from the center point at regular interval of $2\pi/30$ radians. These lines are used as a reference by the experts to click-in the points on the kidney boundary. The angle defined for the formation of straight line is fixed at $2\pi/30$ radians to minimize the expert maneuver in selection of points. This set of twelve points is interpolated to get a smooth contour. The templates created by above procedure may be added with two control points for manually adjusting the template to match the kidney boundary which is then deformed by using MRFs. In *i*-HSIC method, expert clicks on the center along with $10 - 15$ points on the visible portion of kidney boundary. To this extent experts are not biased to click at specified uniformly spaced points as in the case of MRFC scheme. If these points are connected by interpolation then it may appears to be a simple method of contour formation. Also such contour will not correlate well with EOC for most of the cases. Hence certain improvements are made in the proposed method by defining homogeneous

coordinates of points and the order of B-spline interpolation to guarantee optimum contour for different categories of kidney. There is no restriction in the number of points selected, but to standardize the procedure and to minimize the expert maneuver lower and upper limits are defined.

It is understood that number of points selected by the experts are not sufficient for all intra and inter category of kidney. The possible solution is to up-sample the points. As these points are available within the discrete space they may be expressed in polar coordinates [18], as defined by the vectors C(x,y) and θ(x,y), which denote moduli and phases, respectively. The up-sampling may be performed by translating the polar coordinate representation to uniform or homogenous coordinate representation. In the first method the phases are uniformly distributed in a range of 2π radians, whereas in the second method, the area enclosed within the every angular sector are homogeneously distributed over the range of 2π radians. In the former method the points closer to the center are closer to each other and the points farther from the center are more separated. In the latter case the points farther from the center point are closer to each other and those points located closer to the center are angularly more separated, so that the areas of successive angular sectors are equal. The problem associated with the former method is that as contour points are more separated at steep edges the contour formed may not have sufficient smoothness. This shortcoming has been resolved in latter method, where adequate points are available to form smooth contour at bending edges. Once the upsampling of points in homogeneous coordinate is made, these points are connected by higher order spline interpolation technique to form a smooth contour [19 – 21].

If these available points are regarded as a discrete signal $f(k)$, now it become necessary to estimate the intermediate signal values to consider the contour as a continuum $f_c(x)$ rather than a discrete array of pixel coordinate. Many researchers have used the splines for this purpose [22, 23]. A polynomial spline of degree *n* is a piecewise polynomial function of degree *n* with pieces that are patched together to guarantee the continuity of the function and its derivative up to the order *n-1*. Every n^{th} order spline $f_c^n(x)$ can be represented by the expansion,

$$f_c^n(x) = \sum_{k=-\alpha}^{\alpha} c(k)\beta^n(x-k), \ \forall x \in R \qquad (1)$$

where the $c(k)$ are called B-spline coefficients. The basis functions $\beta^n(x-k)$ are the integer shifts of the separable B-spline $\beta^n(x)$ and 'R' is the notation for real number. The B-spline of a higher order *n* can be defined by an explicit expression,

$$\beta^n(x) = \frac{1}{n!}\sum_{k=0}^{n+1} C_k^{n+1}(-1)^k \left(x + \frac{n+1}{2} - k\right)_+^n \qquad (2)$$

Here C_k^{n+1} are the binomial coefficients and the function x_+ is defined as follows

World Academy of Science, Engineering and Technology
International Journal of Electronics and Communication Engineering
Vol:2, No:1, 2008

$$x_+ = \begin{cases} x & \text{for } x > 0 \\ 0 & \text{otherwise} \end{cases} \qquad (3)$$

In most of the spline related works, the splines of order 3 (Cubic B-spline) have been used since they appear to be particularly popular among the researchers for interpolation in general [24]. Using this process, a series of unique cubic polynomials are fitted between each data points, with a demand that the contour obtained be continuous and appear smooth. But the primary reason for working with higher order splines is because of their shortest function with an order of approximation, which in turn provides better support length, L=n+1. The support length may be defined as the maximum distance of separation between successive knots or points. This short support (short function with better support length) property is also a key consideration for computational efficiency. Also splines tend to perform better and better in terms of smoothness as order increases. By increasing the order, splines representation swap from the simplest piecewise constant (n=0) and piecewise linear (n=1) to the other extreme, which corresponds to a band limited signal model (n→+α). The decision regarding the extent to which order can be increased to form a smooth contour has to be identified and same must be implemented.

This is carried out by an estimation of the simple coordinate distance measured between *i*-HSIC contours of different order as given by,

$$d(C_A, C_B) = \sum_{i=1}^{k} \sqrt{(x_i - a_i)^2 + (y_i - b_i)^2} \qquad (4)$$

where C_A and C_B are the contours obtained for order n=P and n=Q

x,y are ordered pair of coordinates of C_A

a,b are ordered pair of coordinates of C_B

i being the number of ordered pair of coordinates, i=0,1,....,k

The distance obtained for order 3 and 5 is 246.66, for order 5 and 7 is 98.34, for order 7 and 9 is 0.00 and for order 9 and 11 is 0.00. These results indicate any further increase in order above 7 of the splines become insignificant. Therefore in the present work, the B-splines of order 7 have been employed.

C . Contour Validation

The comparison and validation of segmentation schemes using standardized protocols becomes necessary to evaluate the performance of the contours. This is to be done for entire images to test the hypothesis that the segmentation output is not statistically different from the gold standard (EOC). For this purpose the parameter derived from the contours such as area enclosed or perimeter may be compared or the property of the region enclosed using statistical, texture and power spectral parameters may be compared or the contours themselves may be compared directly. In first two cases, the resultant value of parameters is application dependant and often the accuracy of measuring these parameters is the functional goal of image segmentation. Hence comparing the contour directly will provide a more definite evaluation. Three such metrics namely maximum coordinate distance '$D_{max}(c_i,c_j)$', mean radial distance 'μ_{rd}' and Hausdorff distance

'$e(C_1, C_2)$' have been used to compare the contours, MSMC, MRFC and *i*-HSIC with EOC. The validation of *i*-HSIC is made based on the result obtained by this comparison.

As mentioned in section II B, the contour can be defined as a series of points in polar coordinate and therefore can be represented by a vector C = {$c_1,c_2,c_3....,c_L$}, where L is the number of points in the contour. Each 'c' is an ordered pair of the x and y coordinates of a point on the contour. Using this vector notation the three metrics are evaluated.

The coordinates of a particular point c_p in the contour is taken as a reference initially and distant measure 'd' is estimated between c_p and all the points c_q. This process is repeated until all the points have been considered as reference. This will result in 'p' maximum distance measures. The coordinates of the points that are dislocated farthest is then obtained by finding the maximum of 'p' maximum values. The maximum coordinate distance '$D_{max}(c_i,c_j)$' as given Eq.(5).

$$D_{max}(c_i, c_j) = \max\left[\max_p \{ d(c_p - c_q) \} \right] \qquad (5)$$

where c_i and c_j are the coordinates of the points that are dislocated farthest

p,q = 1,2,3,.....L

In other two metrics instead of measuring distance between the points, the distance between the contours is estimated. The mean radial distance 'μ_{rd}' between the contours is defined by first choosing a common centroid of the two contours from which radial lines are drawn projecting outward. The intersection of these radial lines with the two contours defines the corresponding points and the metric termed as 'μ_{rd}' is used to estimate the dislocation distance between the contours [25] as in Eq. (6). If two contours are represented by vectors C_1={$c_{11},c_{12},c_{13}....,c_{1L}$}, and C_2={$c_{21},c_{22},c_{23}....,c_{2L}$}, then '$\mu_{rd}$' is defined by,

$$\mu_{rd} = \frac{1}{K} \sum_{i=1}^{K} \left| r_{C_1}\left(i\,2\pi/K\right) - r_{C_2}\left(i\,2\pi/K\right) \right| \qquad (6)$$

where r_{C_1} and r_{C_2} are the radial distance from common centroid to the coordinates of two contours and K is the number of points in the contour.

In Hausdorff distance '$e(C_1, C_2)$' initially the distance to the closest point c_{1i} to the contour C_2 is calculated as

$$d(C_{1i}, C_2) = \min_j \| C_{2j} - C_{1i} \|$$

and the distance to the closest point c_{2i} to the contour C_1 is measured as

$$d(C_{2j}, C_1) = \min_i \| C_{1i} - C_{2j} \|$$ then '$e(C_1, C_2)$' between the two contours is defined as the maximum of the distance to the closest points between the two contours [26] and it is given by

$$e(C_1, C_2) = \max\left(\max_i \{ d(C_{1i}, C_2) \}, \max_j \{ d(C_{2j}, C_1) \} \right) \qquad (7)$$

World Academy of Science, Engineering and Technology
International Journal of Electronics and Communication Engineering
Vol:2, No:1, 2008

The metrics of Eqn. (5), (6) and (7) are used to perform comparative study on contours to evaluate the performance of *i*-HSIC.

III. RESULTS

The formation of EOC by the individual expert illustrates serrated variation in contour due to the motion artifact. This irregularity increases with the mental or physical bias of the expert. The contour has become smooth with minimum fluctuation by using the averaging procedure. The EOC and MSMC attained for three classes of kidney are shown in the Fig. 2. For NR, both the contours are in good agreement, whereas in case of MRD, the MSMC inflate excessively due the insufficient image gradient at the boundary. In cortical polycystic case, the locating the initial seed contour for inflation determines the contour formation. When initial seed contour is located at cystic and non-cystic region, the MSMC totally fails to encapsulate the entire kidney as observed in Fig.2c and this leads to the formation of contours that disagree with EOC. For 78% of NR images, the contours formed by EOC and MSMC show appreciable similarity.

similarity with EOC whereas 40% of MSMC inflate excessively due to lack of image gradient and in 28% of MSMC, some part of contour is fairly correct, some areas get rapt inside the inner structure and in some region it inflate excessively. MSMC completely fails in the region of cysts, only in 36% of polycystic cases where cystic area in pixel is less than 140, MSMC agrees with EOC. The MRFC results from deformation of predefined template and this takes place within the specified deformation zone interval. Table I enumerate the settings of eight parameters to achieve MRFC. For all three kidney classes, the number of sweeps (N_s) with simulated annealing (SA) algorithm is 200. The number of rays (J) drawn from the template contour center point varies from 60 to 70. Each ray is discretized into K points. The number of points (K) per ray is 15 and the deformation zone interval is given by d_{rmax} = 20 pixels in all three cases. The vector of posterior parameters of the energy function ϑ^p that includes probabilistic features namely prior model parameters (ϑ^1, ϑ^2) and likelihood parameters (ϑ^3, ϑ^4) are also given.
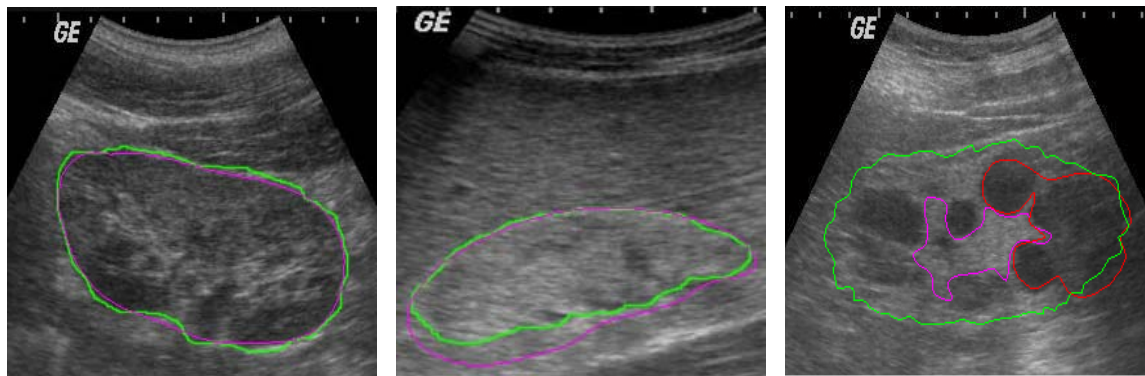

Fig. 2. Contours obtained by EOC and MSMC for three classes of kidney a. Normal Image b. Medical renal diseases c. cortical poly cystic disease. ▬▬▬ EOC; ▬▬▬ MSMC; ▬▬▬ MSMC. In both MSMC initial seed contour is selected within the enclosed region.
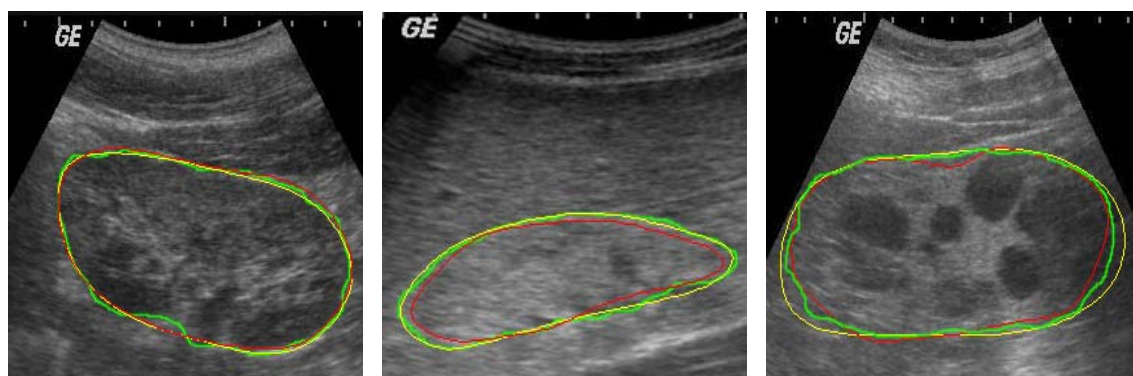

Fig. 3. Contours attained by using EOC, *i*-HSIC and MRFC segmentation schemes for three classes of kidney a. Normal Image b. Medical renal diseases c. cortical poly cystic disease. ▬▬▬ EOC; ▬▬▬ *i*-HSIC; ▬▬▬ MRFC

In 22% of cases due insufficient image gradient at interior and exterior region of boundary, MSMC fails to fit well with EOC. For MRD images, 32% of MSMC shows better

The limitation of MRFC is obvious from Table 1 that certain parameters have to be manually adjusted for each image before the deformation of template. Even though the selection of initial coordinates is subjective in *i*-HSIC method,

World Academy of Science, Engineering and Technology
International Journal of Electronics and Communication Engineering
Vol:2, No:1, 2008

fine tuning of any such parameters is not been involved. The EOC, *i*-HSIC and MRFC formed for NR, MRD and CC kidney images is shown in the Fig. 3.

TABLE I
INITIALIZATION VALUES OF THE PARAMETERS TO OBTAIN
MRFC FOR THREE KIDNEY CATEGORIES

Kidney Category	N_S	J	K	d_{rmax}	$\vartheta^p = \left(\vartheta^1, \vartheta^2, \vartheta^3, \vartheta^4 \right)$
NR	200	60-70	15	20	30-35; 25-35; 25-30; 35-40
MRD	200	75	15	20	30-35; 30-35; 25-30; 35-40
CC	200	75	15	20	30-40; 30-35; 30-35; 35-40

IV. DISCUSSION

The results of MSMC obtained for MRD and CC kidney images suggest that MSMC fail in most of the cases and not suitable for segmentation of different classes of kidney. This indicates automatic segmentation schemes reported in the literatures may not perform favorably. Because the interior region of kidney is not homogenous and often sufficient image gradient with surrounding tissues is not noticed. In some scans, the kidney region is partially occluded. Above all, the posed problem deals with different kidney classes, wherein sonographic visualization confirms anatomical variation in tissue characteristic. Hence automatic contouring procedures that are based on local or global features may not attend to sonographic variations in intra and inter kidney classes.

Referring to the Fig.3, though the resultant MRFC agrees with both EOC and *i*-HSIC fine adjustment (refer Table 1, range of values may be noticed for certain parameters) of 'J' and posterior parameters is necessary before deformation to achieve optimum contour. This makes the procedure more subjective and time consuming. But after setting the parameters the contour formation takes on an average of 0.6 seconds. The reasons for this manual adjustment includes the variation in sonographic visualization of each US kidney image, unclear visual inspection of kidney boundary due to occlusion, dissimilarity in brightness and contrast level of each image because of the variation in setting of scanning system parameters. The failure of MSMC and biased setting of the parameters in MRFC suggests the inferior performance of the methods in segmenting the kidney region.

To evaluate the performance of *i*-HSIC and MRFC with respect to EOC three metrics Dmax(c_i, c_j), μ_{rd} and $e(C_1, C_2)$ are calculated. If C_a, C_b and C_c represent EOC, *i*-HSIC and MRFC respectively, the metrics computed for NR, MRD and CC images are shown in the Fig. 4 and 5. It can be seen that mean, maximum and minimum values of maximum coordinate distance for three contours are almost same. Based on this similarity it cannot be concluded that *i*-HSIC and MRFC correlate with EOC. Because this metric cares only the two coordinates points in the contour for the estimation of distance.
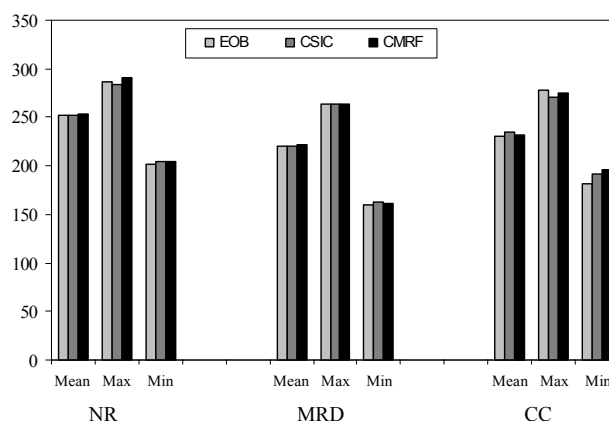

Fig. 4. The maximum co-ordinate distance Dmax(c_i, c_j) obtained for contours C_a(EOC), C_b (*i*-HSIC), and C_c(MRFC) of three kidney classes.

The estimation of mean radial distance 'μ_{rd}' and Hausdorff distance '$e(C_1, C_2)$' shows *i*-HSIC agrees well with EOC. By referring the Table II and Fig.5, the μ_{rd} and $e(C_1, C_2)$ between C_a and C_b is comparably lesser than between C_a and C_c. Even for a worst case CC image the maximum value of 'μ_{rd}' is 5.9727 between C_a and C_b whereas it is 17.8588 for C_a and C_c. Also $e(C_1, C_2)$ is 29.0902 for C_a and C_b and 77.6505 for C_a and C_c. This indicates *i*-HSIC has better correspondence with EOC when compared to MRFC in all three cases of US kidney images. Based on these results it is understood that *i*-HSIC method is superior for the situation where different kidney categories are considered. The US kidney images that are segmented using *i*-HSIC scheme may be made available for further analysis to extract content descriptive features. If such features exist then developing a CAD system that provides certain possibilities like (i). establishing a quantitative universal reference for the US kidney images, (ii). implementing image retrieval in medical application (IRMA) system, (iii). making comparative study on images for objective decision, (iv). developing an expert system that automatically recognizes the extent of pathology or normality, (v). examining extent of healing or failure under post-therapy observation may be realized in practice.

V. CONCLUSION

The implementation of the general segmentation procedure for US kidney images has been dealt to obtain a semi-automated reliable contour. In this paper, three different classes of varied anatomical tissue representation is been considered. The results obtained reveal that MSMC fails in most of MRD and CC cases. The MRFC provide better contour that perform comparably well with EOC but subjective parameters setting in each case influence the reliability in obtaining contour in term of the quality and time. Though a partial objectiveness is involved in acquiring boundary by selecting initial contour coordinate, the *i*-HSIC method provides contour that agrees well with the EOC. To conclude, the investigation on various segmentation schemes suggest that *i*-HSIC may be more suitable to contour kidney

World Academy of Science, Engineering and Technology
International Journal of Electronics and Communication Engineering
Vol:2, No:1, 2008

region of different categories irrespective of wide variation in size, orientation and gray level distribution. Also the proposed scheme explores various possibilities in implementing specific CAD system for US kidney images.
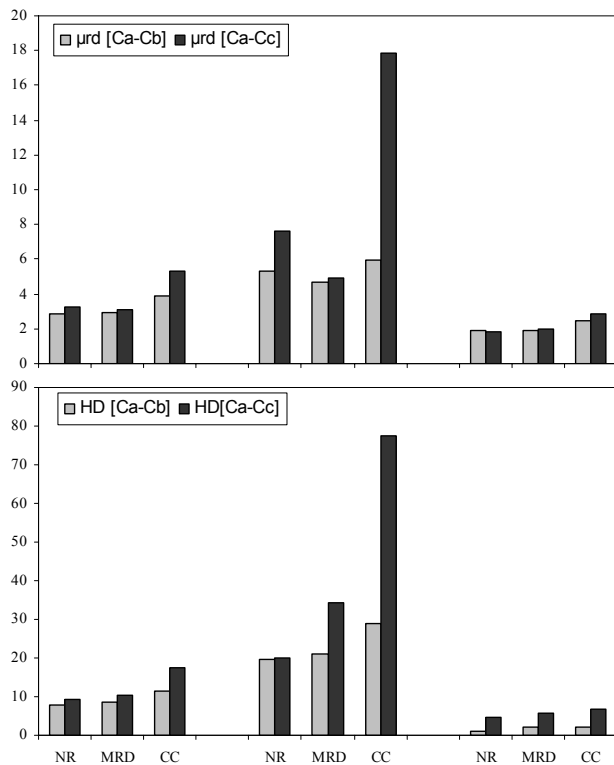

Fig. 5. The mean radial distance 'μrd' and Hausdorff distance 'HD' computed between contours Ca (EOC), Cb (i-HSIC) and Ca (EOC) and Cc (MRFC)

TABLE II
RESULTS OBTAINED FOR VALIDATION METRICS μ$_{RD}$ AND $e(C_1, C_2)$
C$_a$ – EOC; C$_b$ – i-HSIC; C$_c$ – MRFC

Kidney Category	Validation Metrics			
	μ$_{rd}$		$e(C_1, C_2)$	
	C$_a$ – C$_b$	C$_a$ – C$_c$	C$_a$ – C$_b$	Ca – C$_c$
	Mean			
NR	2.8682	3.263	7.9080	9.1318
MRD	2.9633	3.0704	8.5870	10.4561
CC	3.8991	5.3124	11.5995	17.6534
	Maximum			
NR	5.3238	7.6162	19.805	19.8374
MRD	4.6756	4.9496	21.0678	34.4591
CC	5.9727	17.8588	29.0902	77.6505
	Minimum			
NR	1.6381	1.7952	1	4.7626
MRD	1.9101	2.0013	2.2361	5.725
CC	2.4619	2.8839	2	6.7544

REFERENCES

[1] Hagen – Ansert S, (1995), 'Urinary System, In: Diagnostic Ultrasound', 4th edition, St. Louis, MO: Mosby/Elsevier.
[2] H.M.Pollack and B.L.McClennan, (2000), 'Clinical Urography', 2nd Edition, Philadelphia: W. B. Saunders/Elsevier.
[3] Sheng-Fang Huang, Ruey-Feng Chang, Dar-Ren Chen and Woo Kyung Moon, (2004): 'Characterization of Speculation on Ultrasound Lesions', IEEE Trans. on Medical Imaging, 23, pp. 111-121.
[4] C.P.Loizou, C.Christodoulou, C.S.Pattischis, R.S.H.Istepanian, M.Pantziaris and A.Nicolaides, (2002):'Speckle Reduction in Ultrasound Images of Atherosclerotic Carotid Plaque', Proc. 14th IEEE Intl. Conf. on Digital Signal Processing, Santorini, Greece, pp. 525 – 528.
[5] C.P.Loizou, C.S.Pattischis, R.S.H.Istepanian, M.Pantziaris, T.Tyllis and A.Nicolaides, (2004): 'Quality Evaluation of Ultrasound Imaging in the Carotid Artery', Proc. 12th IEEE Mediterranean Electrotechnical Conference, Dubrovnik-Croatia, pp. 395 – 398.
[6] A.Ahumada and C.Null, (1993): 'Image Quality: A Multidimensional Problem', Digital Images and Human Vision, Branford press: Cambridge Mass.
[7] Bakker, J.,Olree, M., Kaatee, R., de Lange, E.E. and Beek, R.J.A., (1997): 'Invitro Measurement of Kidney Size: Comparison of Ultrasonography and MRI', Ultrasound Med. Biol. 24, pp. 683 – 688.
[8] Matre, K., Stokke, E.M., Martens, D. and Gilja, O.H., (1999): 'Invitro Volume Estimation of Kidneys using 3-D Ultrasonography and a Position Sensor', Eur. J. Ultrasound, 10, pp. 65 – 73.
[9] Jain, A.K., Zhong and Y., Lakshmanan, S., (1996): 'Object Matching using Deformable Templates', IEEE Trans. Patt. Anal. Mach. Intell., 18, pp. 267 – 278.
[10] Jun Xie, Yifeng Jiang and Hung-tat Tsui, (2005): 'Segmentation of Kidney from Ultrasound Images Based on texture and Shape Priors', IEEE Trans. on Medical Imaging, 24 , pp. 45 – 57.
[11] Marcos Martin-Fernandez and Carlos Alberola-Lopez, (2005): 'An Approach for Contour Detection of Human Kidney from Ultrasound Images using Markov Random Fields and Active Contours', Medical Image Analysis, 9, pp. 1 – 23.
[12] Abouzar Eslami, Shohreh Kasaei and Mehran Jahed, (2004): 'Radial Multiscale Cyst Segmentation in Ultrasound Images of Kidney', Proc. 4th IEEE International Symposium on Signal Processing and Information Technology, Rome, Italy, pp. 42 – 45.
[13] A.Eslami, M.Jahed and M.Naroienejad, (2005): 'Fully Automated Cyst Segmentation in Ultrasound Images of Kidney', Proc. 3rd IASTED Intl. Conf. on Biomedical Engineering, Austria, PaperID -19418.
[14] Vikram Chalana and Yongmin Kim, (1997): 'A Methodology for Evaluation of Boundary Detection Algorithms on Medical Images', IEEE Trans. on Medical Imaging, 16, pp. 642 – 652.
[15] Kass, M., Witkin, A., and Terzopoulos, D., (1988): 'Snakes: Active Contour Models', Intl. J. Comp. Vis., 1, pp. 321 – 331.
[16] Cohen, L.D., (1991): 'On Active Contour Models and Balloons', CVGIP - Image Understanding, 53, pp. 211 – 218.
[17] Marcos Martin and Carlos Alberola, (2002): 'A Bayesian Approach to Invivo Kidney Ultrasound Contour Detection Using Markov Random Fields', Proc. 5th Intl. Conf. on Medical Image Computing and Computer-Assisted Intervention, Tokyo, Japan, pp. 397 – 404.
[18] Friedland, N.S., and Rosenfeld, A., (1989): 'Ventricular Cavity Boundary Detection from Sequential Ultrasound Images using simulated Annealing', IEEE Trans. Medical Imaging, 8, pp. 344 – 353.
[19] T.M.Lehmann, C.Gonner and K.Spitzer, (1999): 'Survey: Interpolation Methods in Medical Image Processing', IEEE Trans. on Medical Imaging, 18, pp. 1049 – 1075.
[20] M.Unser, (1999): 'Splines: A perfect fit for Signal and Image Processing', IEEE Signal Processing Magazine, 16, pp. 22 – 38.
[21] C. de Boor, (1978): 'A Practical Guide to Splines', New York: Springer-Verlag.
[22] M.Unser, A.Aldroubi and M.Eden, (1993): 'B-Spline Signal Processing: Part I – Theory', IEEE Trans. on Signal Processing, 41, pp. 821 – 833.
[23] M.Unser, A.Aldroubi and M.Eden, (1993): 'B-Spline Signal Processing: Part II – Efficient Design and Applications', IEEE Trans. on Signal Processing, 41, pp. 834 – 848.
[24] Bojan Vrcelj and P.P.Vaidyanathan, (2001): 'Efficient Implementation of All-Digital Interpolation', IEEE Trans. on Image Processing, 10, pp. 1639 – 1646.

World Academy of Science, Engineering and Technology
International Journal of Electronics and Communication Engineering
Vol:2, No:1, 2008

[25] M.Helbing, L.Kahi, C.Rothlubbers and R.Orgimeister, (1997): 'A Reliable Algorithm for Automatic Contour Estimation in Medical Ultrasonic Images of Human Heart', Proc. 4th Intl. Workshop on Systems, Signals and Image Processing, Poznan, Poland, pp. 141 – 144.

[26] D.P.Huttenlocher, G.A.Klanderman and W.J. Rucklidge, (1993): 'Comparing Images using Hausdorff Distance', IEEE Trans. Patt. Anal. Mach. Intell., 15, pp. 850 – 863.

K.Bommanna Raja obtained his BE degree in Electronics and Communication Engineering from Madras University in 1991. He started his career as Lecturer. He received his MTech degree in Bio-Medical Engineering from Indian Institute of Technology (Madras), Chennai. He is working in PSNA college of Engineering and Technology, Dindigul, India, as an Assistant Professor in the Department of Electronics and Communication Engineering. Also as a Head-in-charge, he is engaged in establishing Bio-Medical Engineering Department. Presently he is involved in developing a Computer-Aided Diagnosis system for Ultrasound Kidney Images. He has published more that fifteen research papers in international conferences and journals. His special areas of interest are Medical Imaging, Bio-Signal Processing and Applications of Soft Computing in Image Analysis. He is a member of IEEE (USA), life member of ISTE, IETE and IE (India). He has also coordinated AICTE and ISTE sponsored SDP and STTP programme organized by the Department.

M.Madheswaran received the BE Degree from Madurai Kamaraj University in 1990, ME Degree from Birla Institute of Technology, Mesra, Ranchi, India in 1992, both in Electronics and Communication Engineering. He obtained his PhD degree in Electronics Engineering from the Institute of Technology, Banaras Hindu University, Varanasi, India, in 1999.

At present he is a Principal of Muthayammal Engineering College, Rasipuram, India. He has authored over forty five research publications in international and national journals and conferences. His areas of interest are theoretical modeling and simulation of high-speed semiconductor devices for integrated optoelectronics application, Bio-optics and Bio-signal Processing. He was awarded the Young Scientist Fellowship (YSF) by the State Council for Science and Technology, TamilNadu, in 1994 and Senior Research Fellowship (SRF) by the Council of Scientific and Industrial Research (CSIR), Government of India in 1996. Also he has received YSF from SERC, Department of Science and Technology, Govt. of India. He is named in Marquis Who's Who in Science and engineering in the year 2006. He is a life member of IETE, ISTE and IE (India) and also a senior member of IEEE.

K.Thyagarajah was born in the year 1952. He pursued his BE degree in Electrical and Electronics Engineering from PSG College of Technology, India, in 1976 and ME degree in Power Systems Engineering from College of Engineering, Guindy, Madras, India, in 1979. He obtained his PhD degree from Indian Institute of Science, Bangalore, India, in 1992.

He started his teaching profession as Lecturer at MIT, Manipal, India in 1979. He served at Regional Engineering College, Surathkal, India as Lecturer and Assistant Professor from 1980 to 1995. He joined as Vice-principal in KSR College of Technology, India, in 1995. At present he is heading PSNA college of Engineering and Technology, Dindigul, India as Principal. He has delivered number of special lectures in various reputed institutions. He has published nearly thirty six research papers in international journals and conferences. His fields of interest are Power Electronics, AC Motor Drives, Simulation of Power Converters and Bio-medical Instrumentation.